

## ORIGINAL ARTICLE

# A mutation in FRIZZLED2 impairs Wnt signaling and causes autosomal dominant omodysplasia

Howard M. Saal<sup>1</sup>, Cynthia A. Prows<sup>1,2</sup>, Iris Guerreiro<sup>1</sup>, Milene Donlin<sup>1</sup>, Luke Knudson<sup>1</sup>, Kristen L. Sund<sup>1</sup>, Ching-Fang Chang<sup>3,4</sup>, Samantha A. Brugmann<sup>3,4</sup> and Rolf W. Stottmann<sup>1,3,\*</sup>

<sup>1</sup>Division of Human Genetics, <sup>2</sup>Division of Patient Services, <sup>3</sup>Division of Developmental Biology and <sup>4</sup>Division of Plastic Surgery, Cincinnati Children's Hospital Medical Center, 3333 Burnet Avenue, MLC 7016, Cincinnati, OH 45229, USA

\*To whom correspondence should be addressed. Tel: +1 5136367136; Fax: +1 5136364373; Email: rolf.stottmann@cchmc.org

## Abstract

Autosomal dominant omodysplasia is a rare skeletal dysplasia characterized by short humeri, radial head dislocation, short first metacarpals, facial dysmorphism and genitourinary anomalies. We performed next-generation whole-exome sequencing and comparative analysis of a proband with omodysplasia, her unaffected parents and her affected daughter. We identified a *de novo* mutation in *FRIZZLED2* (*FZD2*) in the proband and her daughter that was not found in unaffected family members. The *FZD2* mutation (c.1644G>A) changes a tryptophan residue at amino acid 548 to a premature stop (p.Trp548\*). This altered protein is still produced *in vitro*, but we show reduced ability of this mutant form of *FZD2* to interact with its downstream target *DISHEVELLED*. Furthermore, expressing the mutant form of *FZD2* *in vitro* is not able to facilitate the cellular response to canonical Wnt signaling like wild-type *FZD2*. We therefore conclude that the *FRIZZLED2* mutation is a *de novo*, novel cause for autosomal dominant omodysplasia.

## Introduction

Autosomal dominant (AD) omodysplasia is a rare skeletal dysplasia characterized by short humeri, dislocated radial head, short first metacarpals, facial dysmorphism with round face, frontal bossing, short nose and long philtrum and variable degrees of genitourinary anomalies. To date, only eight cases have been reported in the literature (1–4), and no reports have identified causative gene mutations. Autosomal recessive (AR) omodysplasia, which differs clinically from the AD form, has also been reported. AR omodysplasia is associated with micro-melia, severe short stature and developmental delays (5). AR omodysplasia is caused by mutations in glypican 6 [*GPC6*; (6)], which is thought to impair WNT5a activity (7,8). Here, we report

a patient with omodysplasia and her similarly affected daughter. Using next-generation exome sequencing, we identify a single causal mutation in the affected patients not present in other family members. Taken together, our sequence analysis, along with our molecular studies, strongly implicates a Wnt-dependent signaling mechanism for AD omodysplasia.

## Results

Patient 1 (proband, Table 1) was born with multiple anomalies, including bilateral cleft lip and cleft palate, short upper extremities, dysmorphic facial features and hypoplastic labia and clitoris. She was the product of a full-term vaginal delivery to a

**Table 1.** Comparison of AD omdysplasia features

Clinical features	Patient 1/ proband	Patient 2	Maroteaux patient 1	Maroteaux Patient 2	Maroteaux Patient 3	Venditti Patient 1	Venditti Patient 2	Gordon patient	Olney Patient 1	Olney Patient 2
Gender	F	F	M	F	F	F	M	F	M	F
Age	25 years	6 years	Newborn	27 years	10 years	12 years	1 month	48 year	23 years	18 months
Stature/length percentile	10	<5	5	10	10	25	25	<5	<5	<5
Skeletal features										
Short humeri	+	+	+	+	+	+	+	+	+	+
Radial dislocation, limitation of movement	+	+	+	+	+	+	+	+	+	+
Short ulnae	NA	+	-	+	+	-	ND	+	-	-
Short first metacarpal	NA	+	+	ND	+	+	+	+	+	+
Femoral anomalies, proximal	NA	+	-	-	+	-	-	+	-	-
Short fibulae	NA	+	-	-	-	-	-	+	-	-
Vertebral anomalies	-	+	-	+	ND	-	-	-	-	-
Craniofacial features										
Round face	+	+	+	ND	+	+	ND	-	ND	ND
Frontal bossing, prominent forehead	+	+	+	+	+	+	+	-	ND	ND
Small nose with broad tip	-	+	+	+	+	+	+	-	ND	ND
Long philtrum	+	+	-	-	+	+	+	+	ND	ND
Flat nasal bridge	+	+	+	ND	+	+	+	-	ND	ND
Cleft lip and cleft palate	+	-	-	-	-	-	-	-	-	-
Genitourinary features										
Hypoplastic genitalia/other genital anomalies	+	-	+	ND	-	+	+	+	ND	ND
Uterine anomalies	+	NA	NR	ND	ND	ND	NR	+	NR	ND

Most common features are highlighted in gray.

NA, not assessed; ND, not described; NR, not relevant.

31-year-old G3P2011 woman and her unrelated 33-year-old husband. The proband's maternal great grandfather was born with cleft lip. Birth weight was 3416 g (80th centile), length 48.3 cm (30th centile) and head circumference 35 cm (70th centile). On her initial evaluation in the Genetics Clinic, she was also noted to have frontal bossing, a flat broad nasal bridge, hypertelorism (interpupillary distance of 45 mm, 97th percentile for age), left preauricular sinus and glabellar hemangiomas, extending from forehead to nasal tip. There was rhizomelic shortening of the upper extremities. Chest and spine X rays, as well as renal ultrasound, were normal. Chromosome analysis showed a normal female karyotype of 46,XX. At the age of 10 years, her height was 132 cm (10th centile), span 103.8 cm, upper-to-lower segment ratio 0.88, head circumference 52.5 cm (50th centile) and interpupillary distance of 5.2 cm (50th centile, Fig. 1A). At 11 years, scoliosis X rays showed a 10 degree dextroscoliosis from T12 to L4 and no vertebral anomalies. During follow-up at 25 years of age (Fig. 1B), she reported a pelvic ultrasound was done to evaluate dyspareunia and a didelphic uterus was identified. Her first pregnancy resulted in the delivery of a male at 22 weeks who expired.

Her subsequent pregnancy resulted in the delivery of a daughter (Patient 2) at 28 weeks of gestation (Fig. 1C).

Patient 2 was the 1130-g product of a twenty-eight 3/7-week vaginal delivery to Patient 1 who was then a 19-year-old G2P0010 woman. The pregnancy was uncomplicated except for maternal use of cigarettes. Patient 2 had respiratory distress syndrome requiring assisted ventilation for 24 h followed by CPAP. The neonatal period was also complicated by grade I intraventricular hemorrhage and feeding difficulties with gastroesophageal reflux. Skeletal X rays showed hypoplasia of T11 vertebral body and bilateral dislocation of the radius with short humeri. At the age of 3 months, she had a round face, mildly dysplastic ears with overfolded helices and apparent hypertelorism (Fig. 2A). The nose was short with a flat nasal bridge, there was a long philtrum and mild micrognathia and the palate was intact. Genitalia appeared normal for a female infant. Follow-up at 6 years revealed that she was healthy with no major medical problems except for recurrent otitis media. Intellectual development was normal, but she was receiving speech therapy in school. Height was 101.2 cm (<second centile), weight 15.6 kg (second centile),

head circumference 49 cm (fifth centile), span was 78.3 cm and upper-to-lower segment ratio was 0.99 (Fig. 2B). Her face was round; nose was short with broad nasal base. There was mild tenting of the upper lip. The ears were posteriorly rotated. The inner canthal distance was 2.9 cm (65th centile), interpupillary distance 5.1 cm (60th centile) and outer canthal distance 8.5 cm (80th centile). The musculoskeletal examination showed

primarily rhizomelic shortening of the upper extremities and a mild shortening of the forearms with limited forearm supination/pronation. There was mild fifth finger clinodactyly with no brachydactyly. The neurologic examination was normal. A skeletal X-ray survey (Fig. 2C–E) showed a dysplastic T11 with anterior wedging and retrolisthesis in relation to T10 and T12. The humeri were short, and poorly formed radial heads were

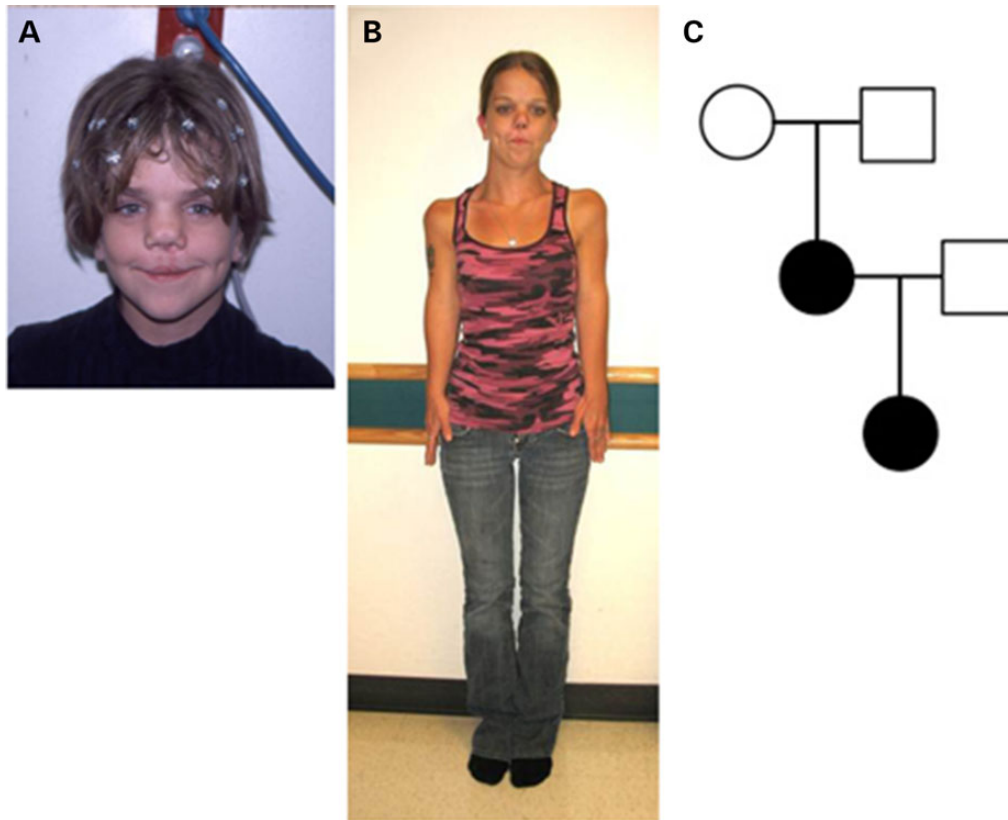


**Figure 1.** Phenotyping of proband and pedigree of patients with AD omodysplasia. Proband at 10 (A) and 25 years of age (B) presenting with skeletal dysplasia and craniofacial phenotypes. The proband's parents and her daughter, represented in the pedigree in (C), provided specimens for exome sequencing.

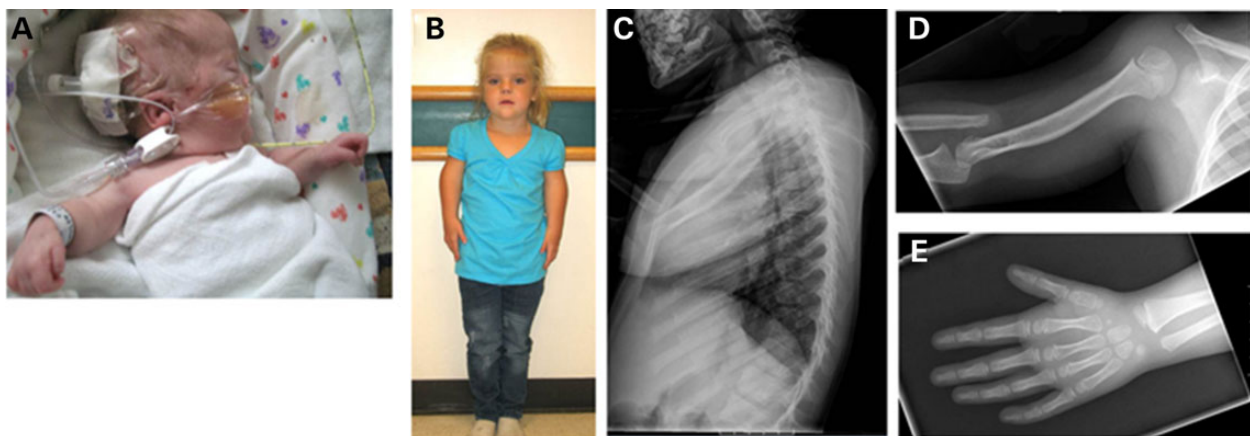


**Figure 2.** Patient 2 with AD omodysplasia. Patient 2 at 3 months (A) and 6 years (B). Skeletal phenotypes include abnormalities of the vertebrae (C), humerus (D) and hands (E).

dislocated bilaterally. The capitella were dysplastic and the ulnas were shortened. The first metacarpals were short. There was widening of the femoral necks and mild lateral uncovering of the femoral heads bilaterally. The fibulas were shortened with hypoplastic proximal ossification centers. There was no additional family history of short stature or limb anomalies.

In order to determine the genetic cause of the dysplasia seen in these patients, we performed next-generation exome sequencing on Patients 1 and 2 as well as the parents of Patient 1. Sheared genomic DNA was enriched with NimbleGen EZ Exome V2 kit, and the exome library was sequenced using Illumina's Hi Seq 2000. Alignment and variant detection was performed using the Broad Institute's web-based Genome Analysis Toolkit [GATK, (9)]. Quality control and data filtering were performed on VCF files in Golden Helix's SNP and Variation Suite. Non-

**Table 2.** Exome sequencing analysis

Familial variant analysis	Number of variants <sup>a</sup>
Total variants	96 485
Quality control	81 617
De novo mutations	8
Coding variants	5
European American variants with MAF < 0.01 (NHLBI ESP6500 exome data)	4
Variants with MAF < 0.01 [1000-genome project (12)]	3
Variants with MAF < 0.01 (internal database)	1

<sup>a</sup>The number of variants identified after exome sequencing and each step of subsequent bioinformatics analysis is indicated. The total analysis indicated only a single mutation that was coding, deleterious and not seen in any control databases.

synonymous coding variants were compared with control databases, including dbSNP, Human Gene Mutation Database, NHLBI's ESP6500 exome data (10), the 1000 Genomes Project (11) and an internal Cincinnati Children's Hospital Medical Center (CCHMC) control cohort. We reasoned the likely mutation was a *de novo* mutation in Patient 1 with AD transmission to Patient 2. Our analysis therefore targeted mutations present only in the affected individuals that were predicted to be deleterious and not present in any of the databases we searched (Table 2). We identified only one such deleterious mutation shared by the proband and affected daughter that was not present in the proband's unaffected parents. A single base pair change (c.1644G>A) within the open reading frame of the gene *FRIZZLED2* (*FZD2*) was identified (Fig. 3A). This nonsense mutation changes a tryptophan residue at amino acid 548 to a premature stop (p.Trp548\*, Fig. 3B). This variant was not found in any control databases. The identified causal p.TRP548\* mutation in Patients 1 and 2 is predicted to result in a truncation of the *FRIZZLED2* protein at the periphery of the canonical *DISHEVELLED* interaction domain, which may have significant consequences for canonical signaling (Fig. 3C). In canonical Wnt signaling, Frizzled binding to Dishevelled requires a conserved motif, KTxxxW, in the intracellular portion of the Frizzled receptor (13–15). The tryptophan residue (W) in the KTxxxW motif is the site of the nonsense mutation in our patients (Fig. 3B). Recent work has shown that the Frizzled–Dishevelled interaction is modulated by a discontinuous motif in Frizzled, which is spread across three intracellular loops of the Frizzled receptor (16). The p.TRP548\* mutation would prevent translation of some of the residues in this model of Dishevelled binding as well.

In support of our finding that omdysplasia is due to a *FZD2* mutation, multiple members of the Wnt pathway are expressed during both limb and craniofacial development in multiple model systems. Previous studies have reported that *Fzd2* is broadly expressed throughout the developing head and limbs in

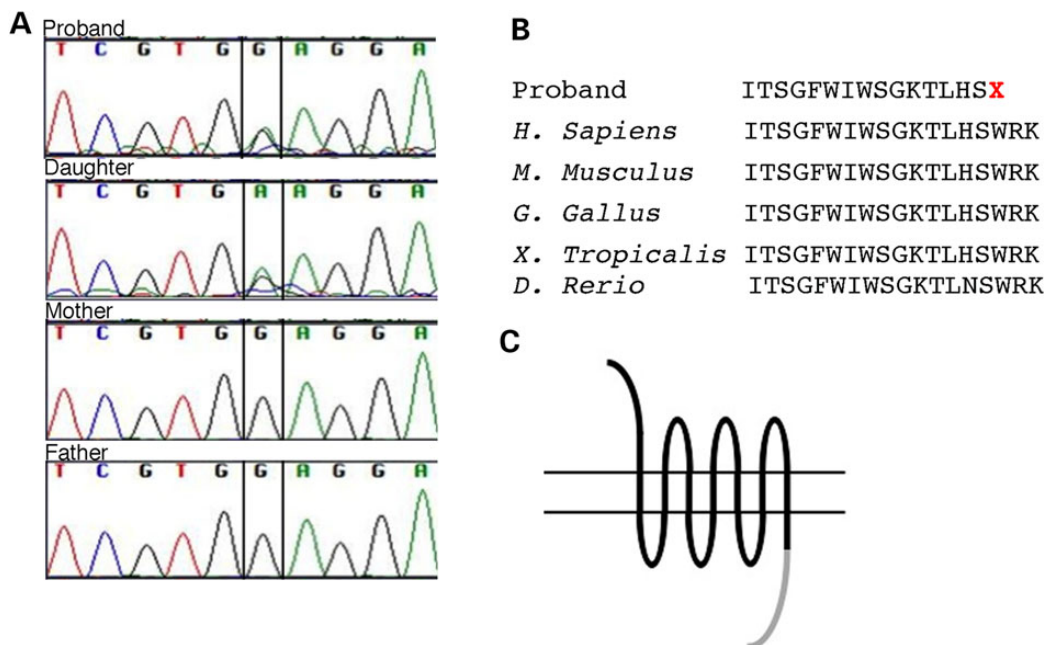


**Figure 3.** Mutations in *FRIZZLED2* cause AD omdysplasia. (A) Sanger sequencing confirms findings from next-generation sequencing of heterozygous *FZD2* mutations in the proband and daughter, but not the proband's parents. (B) *FZD2* mutation creates a premature stop. (C) This is predicted to create an *FZD2* protein lacking the majority of the intracellular cytoplasmic tail partially responsible for Dishevelled binding (gray).



various model systems (17–21). We confirmed these findings by performing *in situ* hybridization for *Fzd2* in an avian model system. *Fzd2* was expressed throughout the developing head (Fig. 4A and B) and within the proximal limb mesenchyme that contributes to the developing skeletal elements (Fig. 4C). Furthermore, FZD2 protein was detected in both the developing head and limb (Fig. 4D). Taken together, our data confirm that of many others and show that the temporal and spatial expression of both *Fzd2* message and FZD2 protein is consistent with the phenotype of omodysplasia. These findings support our hypothesis that mutations in FZD2 could be causal for omodysplasia.

To function as Wnt receptors, Fzd proteins must be properly presented on the cell surface membrane. To determine whether mislocalization of FZD2<sup>p.TRP548\*</sup> was the molecular mechanism associated with AD omodysplasia, we cloned GFP-fusion protein constructs with both wild-type *Fzd2* (*Fzd2*<sup>WT</sup>-GFP) and *Fzd2* with the p.TRP548\* mutation (*Fzd2*<sup>p.TRP548\*</sup>-GFP). There were no observed differences in the subcellular localization of the *Fzd2*<sup>WT</sup>-GFP as compared with the *Fzd2*<sup>p.TRP548\*</sup>-GFP in both HEK293T cells (Fig. 5A and B) and NIH3T3 cells (Fig. 5C and D). Thus, our data suggest that the p.TRP548\* mutation does not affect the stability or subcellular localization of FZD2.

A key component of Wnt signal transduction is the binding of Dishvelled (Dvl) proteins to the intracellular portion of the Fzd receptor upon Wnt ligand binding. As the *Fzd2* p.TRP548\* mutation is predicted to result in loss of some of the Dvl-binding domain, we tested the ability of *Fzd2*<sup>p.TRP548\*</sup>-GFP-mutant protein to recruit Dvl to the plasma upon Wnt activation. A Dvl2-FLAG fusion protein was co-expressed in both HEK293T cells and NIH3T3 cells (data not shown) along with either *Fzd2*<sup>WT</sup>-GFP or *Fzd2*<sup>p.TRP548\*</sup>-GFP-mutant proteins. Prior to Wnt treatment, the Dvl2 protein was largely found in discrete puncta throughout the cell, not co-localizing with the *Fzd2*-GFP-fusion proteins (Fig. 6A–D and I–L). Upon stimulating cells expressing *Fzd2*<sup>WT</sup>-GFP and Dvl2-FLAG with Wnt media, the punctate expression of Dvl2-FLAG was lost and a significant portion of the *Fzd2*<sup>WT</sup>-GFP and Dvl2-FLAG proteins were co-localized (Fig. 6E–H). We next examined cells expressing *Fzd2*<sup>p.TRP548\*</sup>-GFP-mutant protein and Dvl2-FLAG. In the absence of Wnt ligand, Dvl2-FLAG was also expressed in discrete puncta throughout the cell, not co-localizing with the *Fzd2*<sup>p.TRP548\*</sup>-GFP-mutant protein (Fig. 6I–L). In the presence of Wnt however, we saw a significant reduction in the recruitment and persistence of the intercellular puncta, as compared with the changes we noted with *Fzd2*<sup>WT</sup>-GFP (Fig. 6M–P). We quantified these results via measuring both the proportion of cells in each experimental category (no, some or significant (co-localization, Fig. 6Q), as well as determining an average co-localization value for each cell in each treatment (Fig. 6R) and found that a significant co-localization was identified only in the Wnt-treated *Fzd2*<sup>WT</sup>-GFP cells (Fig. 6Q and R). Very little localization was detected in non-treated *Fzd2*<sup>WT</sup>-GFP cells or in *Fzd2*<sup>p.TRP548\*</sup>-GFP cells regardless of Wnt treatment (Fig. 6Q and R). In fact, there was not a significant co-localization or loss of Dvl-positive puncta in any Wnt-treated cells expressing *Fzd2*<sup>p.TRP548\*</sup>-GFP.

We hypothesized that the expression of a prematurely truncated FZD2 protein lacking a portion of the intracellular domain would have a negative effect upon Wnt signaling. In order to assess Wnt-signaling activity, we utilized an *in vitro* signaling system. SuperTOPFLASH (STF) cells stably express a Wnt luciferase reporter controlled by a series of TCF-LEF binding sites known to transduce canonical Wnt signaling and serve as a robust *in vitro* model (22). Expressing *Fzd2*<sup>WT</sup>-GFP in these STF cells resulted in an almost 3-fold increase in Wnt signaling. In striking contrast, expressing *Fzd2*<sup>p.TRP548\*</sup>-GFP in STF cells did not result in any

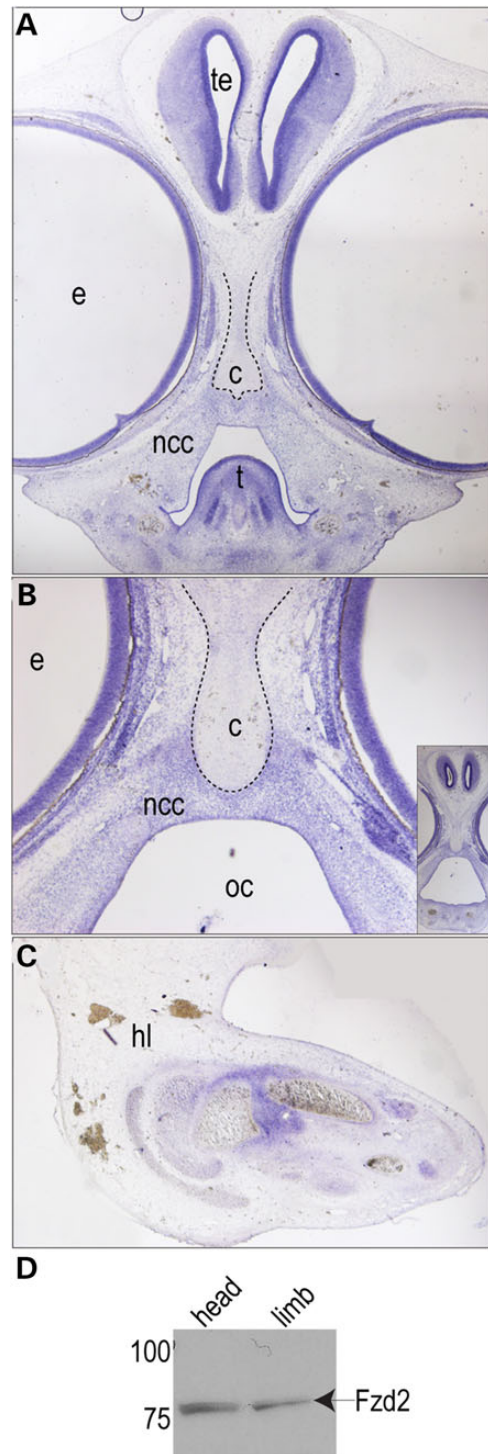


**Figure 4.** *Fzd2* expression in developing craniofacial and limb tissues. RNA *in situ* hybridization indicates the expression of *Fzd2* in HH stage 30 chicken embryos in the developing face (A and B) and limbs (C). Image in B is higher magnification view of image shown in the inset. Digoxigenin-labeled riboprobes were used according to published protocols. (D) Western immunoblotting for FZD2 protein confirms expression in these tissues from HH stage 25 embryos. c-cartilage, e-eye, hl-hindlimb, ncc-neural crest cells, oc-oral cavity, te-telencephalon and t-tongue.

notable increase in Wnt activity over that of background levels (Fig. 7). These data are consistent with a model wherein the FZD2<sup>p.TRP548\*</sup>-mutant protein lacking a portion of the

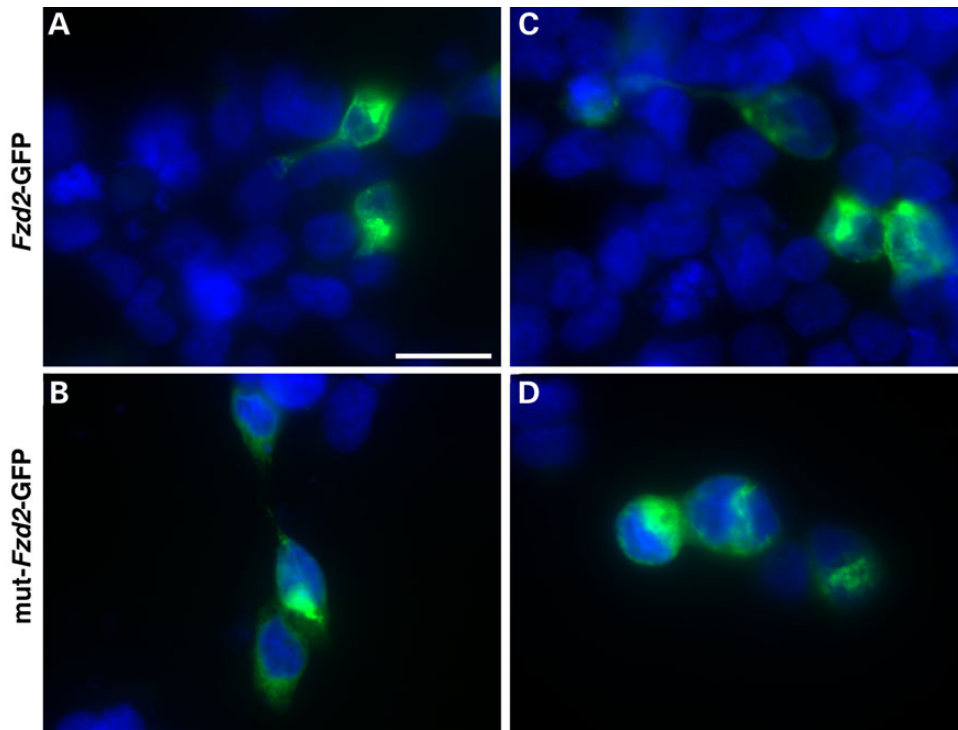


Figure 5. The p.W458X mutation does not alter protein levels or subcellular localization. Expression of either *Fzd2*<sup>WT</sup>-GFP (A and C) or *Fzd2*<sup>p.TRPS48\*</sup>-GFP (B and D) in HEK293T (A and B) or NIH3T3 (C and D) cells does not significantly differ in abundance or subcellular localization. Scale bar is equal to 20  $\mu$ m.

intracellular domain is significantly less efficient in transducing WNT signaling than the wild-type FZD2. Given our data and the genetic pattern of inheritance, we suggest that the patients that carry the p.TRPS48\* are haploinsufficient for FZD2 in skeletal development. Alternatively, the p.TRPS48\* mutation could also be functioning as a 'dominant negative' where the expression of the mutant protein is sufficient to reduce Wnt activity, likely by properly binding Wnt ligand at the surface but not propagating the signal. Either of these hypothesized molecular mechanisms would be consistent with the phenotypes arising in humans with heterozygous, *de novo* FZD2 mutations.

## Discussion

The advent of next-generation whole-exome sequencing has opened up vast new opportunities to identify novel, as well as rare and difficult-to-diagnose, single-gene disorders (23). This in turn has led to identification of new disorders and recognition of previously unrecognized phenotypes from known genes and developmental pathways. This is not only important for an understanding of genetic syndromes and disorders, but also the ability to attach specific genes and gene mutations with a specific phenotype gives us greater insight into these developmental pathways. We report two patients, a mother and daughter with AD omodysplasia, both of whom have a c.1644G>A mutation in the *FZD2* gene, not previously associated with human disease. The availability of Patient 1's unaffected biologic parents greatly facilitated the comparative analysis for exomes. This gene codes for the FRIZZLED2 protein that acts as a Wnt receptor. We show that *Fzd2* is expressed in the developing face and skeleton in multiple model systems (Fig. 4). We further show that the truncated form of the protein mimicking the human mutation is stable (Fig. 5), expressed *in vitro* (Fig. 5), does not interact normally

with Dvl (Fig. 6) and does not properly transduce canonical Wnt signaling (Fig. 7). Regarding our Dvl-interaction experimental system, we do note that in some systems the expression of *Fzd2* alone is sufficient to recruit Dvl to the plasma membrane. In our system (Fig. 6), the addition of Wnt significantly alters the localization of Dvl (i.e. recruits out of the cytoplasmic punctate accumulations to more significantly appear to co-localize with *Fzd2*). This may be due to the differences in cell types used as compared with other systems (XENOPUS animal caps (14,24) and DROSOPHILA cells (25) as compared with mammalian cells *in vitro*) or the relative levels of the expression of experimental components in our assay.

There is significant evidence in the literature supporting our conclusion that *FZD2* is a causal gene for AD omodysplasia. *WNT5A* is a known ligand for *FZD2* and is mutated in patients with AD Robinow Syndrome, which is characterized by mesomelic shortening, short stature, hypertelorism and mandibular hypoplasia (26). Similarly, multiple perturbations of Wnt signaling negatively impact skeletal development in animal models. Truncations in various members of the *Fzd1,2,7* subfamily lead to a delay or block in chondrocyte maturation and shortening of skeletal elements (27,28). Directly relevant to the phenotype and model we present here, retroviral expression of chicken *Fzd1* and *Fzd7* with deletions of intracellular C-terminal domains (24 amino acids) resulted in shortened and bent humeri, shortened ulna and bent radii (27). This deletion almost perfectly mimics the predicted effect of the mutation in our human patients [also see (29)]. Thus, there is ample precedent for disruptions in Wnt signaling leading to skeletal dysplasia similar to those seen in AD omodysplasia.

There is similarly robust evidence that Wnt signaling is crucial for craniofacial development. *WNT3* mutations are found in a human syndrome that includes cleft palate among its

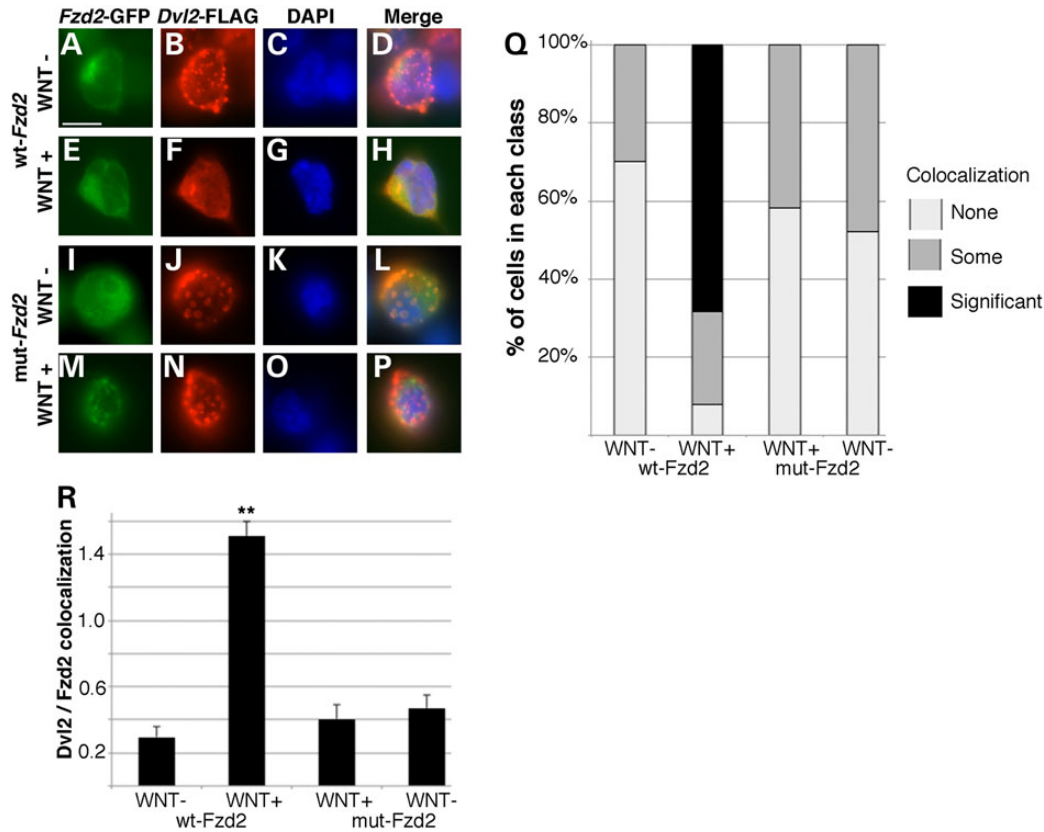


**Figure 6.** Dvl2-Fzd2 interactions are perturbed in cells expressing truncated FZD2. Co-expression of Dvl2-FLAG and either  $Fzd2^{WT}$ -GFP (A-H) or  $Fzd2^{p.TRP548}$ -GFP (I-P) in unstimulated HEK293T cells resulted in accumulations of Dvl2-FLAG puncta throughout the cell. Wnt treatment in  $Fzd2^{WT}$ -GFP cells (E-H) resulted in increased colocalization of the Fzd and Dvl after immunocytochemistry and dissipation of most Dvl2-positive puncta, indicating successful recruitment to the plasma membrane. Treatment of  $Fzd2^{p.TRP548}$ -GFP-mutant cells, however, did not show a robust recruitment of Dvl2-FLAG (M-P). This was quantified as proportion of cells with 'no', 'some' or 'significant' colocalization and loss of puncta (Q) and as an average colocalization value for each cell (R). Number of double-transfected cells analyzed for each condition is indicated in R. Scale bar is equal to 10  $\mu$ m. \*\* $P = 0.001$  versus untreated cells.

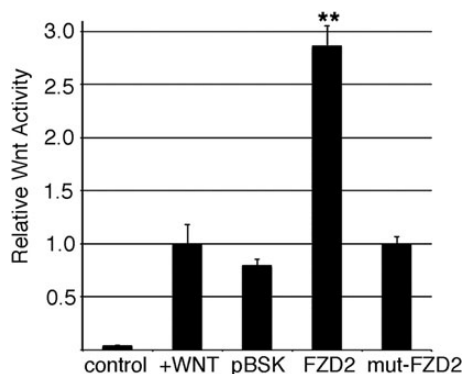


**Figure 7.** Expression of truncated FZD2 attenuates canonical Wnt-signaling. STF Wnt reporter cells were transfected with control plasmids or  $Fzd2^{p.TRP548}$ -GFP (mut-Fzd2) and treated with Wnt-conditioned media. Expression of increasing amounts of  $Fzd2^{p.TRP548}$ -GFP reduced the cellular response to Wnt ligand as measured by luciferase activity. Wnt luciferase activity was normalized to the treated, non-transfected cells. \*\* $P = 0.002$  versus control transfection.

phenotypes (30). Furthermore, the disruption of Wnt signaling via delivery of a Wnt antagonist produces similar midfacial malformations and clefting (31). The phenotypes we note in the AD omodyplaisa patients of frontal bossing, small nose, broad tip,

long philtrum and flat nasal bridge do not necessarily translate as readily to mouse models making it more difficult to evaluate those phenotypes in animal models. However, Fzds and Wnts are often implicated in the more easily appreciated cleft palate phenotype. At least eleven Wnt ligands are expressed in the mouse during stages important for craniofacial development (19) and multiple mutants have craniofacial phenotypes, including Frizzled receptors (32-34).

Of note in Patient 1 was also the presence of bilateral cleft lip with cleft palate. It was noted that Patient 1's great grandfather was born with cleft lip, but there was no additional family history of cleft lip with/without cleft palate. The cleft lip and cleft palate are not likely part of the omodyplaisa phenotype. To identify candidate mutations that may explain why Patient 1 has these craniofacial phenotypes whereas Patient 2 does not, we reexamined the exomes, focusing on genes in Wnt signaling, which had variants in Patient 1 but not her daughter. We found seven variants in five WNT genes for which the genotype of Patient 1 differed from her daughter (Table 3). Patient 1 was homozygous for variants in WNT11 and WNT2B for which the daughter was heterozygous. The proband also had five additional heterozygous variants in WNT16, WNT3A and WNT9A that were absent in her daughter. None of Patient 1's additional variants in WNT genes are predicted to have an extremely high consensus impact in the bioinformatics analysis. Wnt11 and



**Table 3.** Wnt-signaling mutations in patients identified by exome sequencing

Key	Reference allele	Alternate allele	dbSNP ID	dbSNP MAF	Gene	Consensus impact	Proband	Proband's daughter
11_75902539_G_WNT11	A	G	rs11236648	0.239	WNT11	MODIFIER	Homozygous variant	Heterozygous
7_120969769_A_WNT16	G	A	rs2908004	0.4799	WNT16	MODERATE	Heterozygous	No variant
7_120979089_T_WNT16	C	T	rs2707466	0.4716	WNT16	MODERATE	Heterozygous	No variant
1_113063125_G_WNT2B	A	G	rs910697	–	WNT2B	LOW	Homozygous variant	Heterozygous
1_228238333_T_WNT3A	C	T	–	–	WNT3A	MODIFIER	Heterozygous	No variant
1_228112121_G_WNT9A	A	G	rs4653889	0.4863	WNT9A	MODIFIER	Heterozygous	No variant
1_228113163_G_WNT9A	A	G	rs3795768	0.3246	WNT9A	LOW	Heterozygous	No variant

*Wnt2b* are expressed in the mouse pharyngeal arches (35,36), SNPs in *WNT3A* have been associated with nonsyndromic cleft lip and palate (37,38) and *Wnt9a* is required for pharyngeal arch development in the zebrafish (39). While several of the variants are known minor alleles, in the presence of a *FZD2* mutation, one or more of these could potentially explain the presence of the clefting phenotypes in the proband but not the daughter (34).

In addition to canonical, beta-catenin-mediated signaling, Wnts and Fzds also activate a non-canonical/planar cell polarity (PCP) pathway that allows individual cells to sense their relative position within a field. Thus, the phenotypes we see could be due to alterations in both canonical/beta-catenin-mediated and/or non-canonical/PCP-mediated Wnt signaling. Human *FZD2* and chicken *Fzd1/Fzd7* have been shown to activate canonical beta-catenin Wnt signaling (28,40). Our *in vitro* experiments show that the expression of *FZD2*<sup>P.TRP548\*</sup> has little activity in a canonical Wnt activity assay (Fig. 6). However, several experimental results also indicate that PCP signaling may be disrupted. *Fzd2* is concentrated to the leading edge of migrating cells *in vitro* (41). *Fzd9*-mutant mice show defects in matrix mineralization but do not show defects in canonical Wnt signaling (42). In the *Fzd1*<sup>-/-</sup>; *Fzd2*<sup>-/-</sup> mutants with the cleft palate phenotype, microarray analysis showed little differences in the transcriptional profile as compared with wild-type (19). Significant changes in target genes would be predicted if nuclear beta-catenin was regulating the activity of multiple target genes in the palate. The *Fzd1*<sup>-/-</sup>; *Fzd2*<sup>-/-</sup>-mutant embryos also have a wider roof of the mouth, suggestive of a convergent extension phenotype.

Some of the most definitive experiments to correlate *Fzd* activities with either canonical signaling or PCP were performed by Yu and colleagues (34). In canonical Wnt-signaling assays, *Fzd2* was much more active in conjunction with *Wnt3* and *Wnt3a* than *Wnt5a* (canonical and non-canonical ligands, respectively). In parallel experiments to test non-canonical Wnt signaling through co-assembly with *Celsr1* at the membrane surface, *Fzd1*, *Fzd2*, *Fzd7* showed little colocalization suggesting limited PCP pathway activity. Taken together, these results do not allow us to make a definitive determination of which arm of the Wnt-signaling pathway is most affected in *FZD2*-dependent AD omdysplasia. It is most likely that both mechanisms of Wnt signaling are affected to some degree but our data show a clear decrease in canonical Wnt signaling as a result of this mutation.

## Materials and Methods

### Subjects

Informed consent was obtained according to CCHMC institutional review board protocol # 2012-0203. Following consent, blood

was collected on the parents, residual DNA on the affected individuals and spit on the unaffected proband.

### Genotyping

Library generation, exome enrichment, sequencing, alignment and variant detection were performed in the CCHMC Genetic Variation and Gene Discovery Core Facility (Cincinnati, OH, USA). Briefly, sheared genomic DNA was enriched with Nimble-Gen EZ Exome V2 kit (Madison, WI, USA). The exome library was sequenced using Illumina's Hi Seq 2000 (San Diego, CA, USA). Alignment and variant detection was performed using the Broad Institute's web-based GATK.

### Variant filtering and pathogenicity assessment

Quality control and data filtering were performed on VCF files in Golden Helix's SNP and Variation Suite (Bozeman, MT, USA). Non-synonymous coding variants were compared with three control databases, including NHLBI's ESP6500 exome data, the 1000 genomes project and an internal CCHMC control cohort. Remaining variants were subject to AR analysis with emphasis on homozygous recessive variants found in the region of homozygosity identified by SNP microarray. The identified variant was compared with known disease genes in the OMIM and Human Gene Mutation (HGMD) databases and to reported variants in dbSNP and the Exome Variant Server. The *FZD2* mutation was confirmed with Sanger Sequencing (primers: F—GCGTCTTCT CCGTGCTCTAC; R—TACAAACCTTGTGGGGTGT).

### In situ hybridization

Patterns of gene expression in the face and limb of embryos were analyzed via sectioned *in situ* hybridization using digoxigenin-labeled riboprobes as described on the Gallus Expression *in situ* hybridization Analysis site (GEISHA (43,44)). Probe for *FZD2* was designed according to sequences listed on GEISHA.

### Western blot analysis

Facial prominences and developing limbs were dissected from HH 25 chicken embryos. Tissue was rinsed with cold chick salt (127 mM NaCl) twice and sonicated in RIPA buffer (50 mM Tris, 150 mM NaCl, 0.1% sodium dodecyl sulfate, 0.5% sodium deoxycholate and 1% Triton X-100) containing protease and phosphatase inhibitors (Thermo Scientific, #87786, Pittsburgh, PA, USA). Protein concentration was measured by BCA protein assay (Thermo Scientific, #23227, Pittsburgh), and 30 µg protein was applied to a 6% SDS-PAGE gel. Rabbit polyclonal anti-Fzd2 antibody (LSBio, LS-C166295, Seattle, WA, USA).



## Fusion protein expression and immunocytochemistry

The pCD-rFrizzled2-myc expression vector was commercially obtained (Addgene plasmid 16812, R. Moon donation), and the Trp548Stop mutation was recapitulated using the Quik Change II Site Directed Mutagenesis kit (Stratagene). Both constructs were subcloned into the V6 CE.GFPLT CS2+ vector (Addgene plasmid 17097, R. Moon donation) to generate GFP expression constructs for both the wild-type *Frizzled2* and the Trp548Stop mutation. GFP-fusion proteins were visualized directly without further antibody amplification. The Dvl2-FLAG construct was commercially obtained (Addgene plasmid 24802, J. Wrana donation) and visualized with a rabbit anti-FLAG polyclonal antibody (Abcam) and a Alexa-Fluor594 goat anti-rabbit antibody (Life technologies) using 4% paraformaldehyde fixation and standard methods. GFP expression and/or Dvl-FLAG plasmids were transfected into both HEK293T (human) and NIH3T3 (mouse) cells using the Lipofectamine 3000 transfection reagent following manufacturer's instructions.

## Wnt-conditioned media

WNT3A media was collected from cells stably expressing *Wnt3a*. DMEM/FBS was collected in two batches after 4 and 3 days of incubation. These collections were mixed, stored at 4°C and added directly to cells to induce Wnt signaling (so-called treated or stimulated).

## Dvl colocalization experiments

*Fzd2* and *Dvl2* constructs were expressed and imaged as described earlier. Similar to previous reports (15,16,25), 24 h after transfection, cells were either fixed and stained (untreated) or treated with Wnt-conditioned media for 24 h then fixed and stained. Images were collected using a Zeiss ApoTome microscope. After collecting images, *Dvl2/Fzd2* colocalization was determined by three blinded observers. Each cell was determined to have no colocalization (and assigned a value of 0), some colocalization (a value of 1) or significant colocalization (2). Data were analyzed for concordance among observers, and cells were then binned (Fig. 6Q). Additionally, an average colocalization value (0.0–2.0) was determined for each cell from the multiple observers. This average 'Dvl2/Fzd2 colocalization' value was compared among treatments (Fig. 6R). Statistical significance was determined with a Student's t-test (Microsoft Excel).

## Wnt-signaling assay

Assay was performed largely as in previous studies (22,34). STF cells carrying a Wnt-responsive luciferase assay were transfected in a six-well plate with pBSK and/or V6.CE.GFPLT plasmids as controls, *Fzd2*-GFP or *Fzd2*<sup>p.TRP548</sup>-GFP in equal concentrations (60 ng) using Lipofectamine 3000 following manufacturer's protocols. Twenty-four hours after transfection, cells were transferred to 96-well plates at 40 000 cells/well. Six-to-eight hours after 96-well plating, cells were stimulated with Wnt3a-conditioned media or control media, and Wnt activity was measured after 24 h *in vitro* using the Dual-Glo luciferase System (Promega) and manufacturer's protocols. Wnt luciferase activity was normalized to the untransfected, Wnt-treated cells.

## Supplementary Material

Supplementary Material is available at HMG online.

## Acknowledgements

We thank the family members for agreeing to be part of this study and members of the Stottmann laboratory for analysis shown in Figure 6.

*Conflict of Interest statement.* None declared.

## Funding

This study was supported by the Cincinnati Children's Research Foundation Research and Innovation Pilot Award (S.A.B. and R.W.S.). I.G. is a student in the Magistère de Génétique Graduate Program at Université Paris Diderot, Sorbonne Paris Cité.

## References

- Maroteaux, P., Sauvegrain, J., Chrispin, A. and Farriaux, J.P. (1989) Omodysplasia. *Am. J. Med. Genet.*, **32**, 371–375.
- Venditti, C.P., Farmer, J., Russell, K.L., Friedrich, C.A., Alter, C., Canning, D., Whitaker, L., Mennuti, M.T., Driscoll, D.A. and Zackai, E.H. (2002) Omodysplasia: an affected mother and son. *Am. J. Med. Genet.*, **111**, 169–177.
- Gordon, B.L., Champaigne, N.L., Rogers, R.C., Frias, J.L. and Leroy, J.G. (2014) Long-term observation of a patient with dominant omodysplasia. *Am. J. Med. Genet. Part A*, **164A**, 1234–1238.
- Olney, A., Thomas, J., Anderson, R., Murphy, M. and Hasstrom, J. (1990) Autosomal dominant Robinow syndrome with rhizomelic brachymelia. *Proc. Greenwood Genet. Ctr.*, **9**, 72–73.
- Borochowitz, Z., Sabo, E., Misselevitch, I. and Boss, J.H. (1998) Autosomal-recessive omodysplasia: prenatal diagnosis and histomorphometric assessment of the physal plates of the long bones. *Am. J. Med. Genet.*, **76**, 238–244.
- Campos-Xavier, A.B., Martinet, D., Bateman, J., Belluoccio, D., Rowley, L., Tan, T.Y., Baxova, A., Gustavson, K.H., Borochowitz, Z.U., Innes, A.M. et al. (2009) Mutations in the heparan-sulfate proteoglycan glypican 6 (GPC6) impair endochondral ossification and cause recessive omodysplasia. *Am. J. Hum. Genet.*, **84**, 760–770.
- Yiu, G.K., Kaunisto, A., Chin, Y.R. and Toker, A. (2011) NFAT promotes carcinoma invasive migration through glypican-6. *Biochem. J.*, **440**, 157–166.
- Dwivedi, P.P., Lam, N. and Powell, B.C. (2013) Boning up on glypicans—opportunities for new insights into bone biology. *Cell Biochem. Funct.*, **31**, 91–114.
- McKenna, A., Hanna, M., Banks, E., Sivachenko, A., Cibulskis, K., Kernytzky, A., Garimella, K., Altshuler, D., Gabriel, S., Daly, M. et al. (2010) The genome analysis toolkit: a MapReduce framework for analyzing next-generation DNA sequencing data. *Genome Res.*, **20**, 1297–1303.
- Fu, W., O'Connor, T.D., Jun, G., Kang, H.M., Abecasis, G., Leal, S.M., Gabriel, S., Rieder, M.J., Altshuler, D., Shendure, J. et al. (2013) Analysis of 6,515 exomes reveals the recent origin of most human protein-coding variants. *Nature*, **493**, 216–220.
- Genomes Project, C., Abecasis, G.R., Altshuler, D., Auton, A., Brooks, L.D., Durbin, R.M., Gibbs, R.A., Hurles, M.E. and McVean, G.A. (2010) A map of human genome variation from population-scale sequencing. *Nature*, **467**, 1061–1073.
- International HapMap, C., Altshuler, D.M., Gibbs, R.A., Peltonen, L., Altshuler, D.M., Gibbs, R.A., Peltonen, L., Dermitzakis, E., Schaffner, S.F., Yu, F. et al. (2010) Integrating common and

- rare genetic variation in diverse human populations. *Nature*, **467**, 52–58.
13. Djiane, A., Yogev, S. and Mlodzik, M. (2005) The apical determinants aPKC and dPatj regulate Frizzled-dependent planar cell polarity in the Drosophila eye. *Cell*, **121**, 621–631.
  14. Umbhauer, M., Djiane, A., Goisset, C., Penzo-Mendez, A., Riou, J.F., Boucaut, J.C. and Shi, D.L. (2000) The C-terminal cytoplasmic Lys-thr-X-X-X-Trp motif in frizzled receptors mediates Wnt/beta-catenin signalling. *EMBO J.*, **19**, 4944–4954.
  15. Wu, J., Klein, T.J. and Mlodzik, M. (2004) Subcellular localization of frizzled receptors, mediated by their cytoplasmic tails, regulates signaling pathway specificity. *PLoS Biol.*, **2**, E158.
  16. Tauriello, D.V., Jordens, I., Kirchner, K., Slootstra, J.W., Kruitwagen, T., Bouwman, B.A., Noutsou, M., Rudiger, S.G., Schwamborn, K., Schambony, A. et al. (2012) Wnt/beta-catenin signaling requires interaction of the Dishevelled DEP domain and C terminus with a discontinuous motif in Frizzled. *Proc. Natl Acad. Sci. USA*, **109**, E812–E820.
  17. Sisson, B.E. and Topczewski, J. (2009) Expression of five frizzleds during zebrafish craniofacial development. *Gene Express. Patterns*, **9**, 520–527.
  18. Geetha-Loganathan, P., Nimmagadda, S., Antoni, L., Fu, K., Whiting, C.J., Francis-West, P. and Richman, J.M. (2009) Expression of WNT signalling pathway genes during chicken craniofacial development. *Develop. Dyn.*, **238**, 1150–1165.
  19. Yu, H., Smallwood, P.M., Wang, Y., Vidaltamayo, R., Reed, R. and Nathans, J. (2010) Frizzled 1 and frizzled 2 genes function in palate, ventricular septum and neural tube closure: general implications for tissue fusion processes. *Development*, **137**, 3707–3717.
  20. Nohno, T., Kawakami, Y., Wada, N., Komaguchi, C. and Nishimatsu, S. (1999) Differential expression of the frizzled family involved in Wnt signaling during chick limb development. *Cell. Mol. Biol.*, **45**, 653–659.
  21. Visel, A., Carson, J., Oldekamp, J., Warnecke, M., Jakubcakova, V., Zhou, X., Shaw, C.A., Alvarez-Bolado, G. and Eichele, G. (2007) Regulatory pathway analysis by high-throughput in situ hybridization. *PLoS Genet.*, **3**, 1867–1883.
  22. Xu, Q., Wang, Y., Dabdoub, A., Smallwood, P.M., Williams, J., Woods, C., Kelley, M.W., Jiang, L., Tasman, W., Zhang, K. et al. (2004) Vascular development in the retina and inner ear: control by Norrin and Frizzled-4, a high-affinity ligand-receptor pair. *Cell*, **116**, 883–895.
  23. Yang, Y., Muzny, D.M., Reid, J.G., Bainbridge, M.N., Willis, A., Ward, P.A., Braxton, A., Beuten, J., Xia, F., Niu, Z. et al. (2013) Clinical whole-exome sequencing for the diagnosis of mendelian disorders. *New Engl. J. Med.*, **369**, 1502–1511.
  24. Axelrod, J.D., Miller, J.R., Shulman, J.M., Moon, R.T. and Perrimon, N. (1998) Differential recruitment of Dishevelled provides signaling specificity in the planar cell polarity and Wingless signaling pathways. *Genes Develop.*, **12**, 2610–2622.
  25. Simons, M., Gault, W.J., Gotthardt, D., Rohatgi, R., Klein, T.J., Shao, Y., Lee, H.J., Wu, A.L., Fang, Y., Satlin, L.M. et al. (2009) Electrochemical cues regulate assembly of the Frizzled/Dish-evelled complex at the plasma membrane during planar epithelial polarization. *Nat. Cell Biol.*, **11**, 286–294.
  26. Person, A.D., Beiraghi, S., Sieben, C.M., Hermanson, S., Neumann, A.N., Robu, M.E., Schleiffarth, J.R., Billington, C.J. Jr., van Bokhoven, H., Hoogeboom, J.M. et al. (2010) WNT5A mutations in patients with autosomal dominant Robinow syndrome. *Develop. Dyn.*, **239**, 327–337.
  27. Hartmann, C. and Tabin, C.J. (2000) Dual roles of Wnt signaling during chondrogenesis in the chicken limb. *Development*, **127**, 3141–3159.
  28. Li, Y. and Dudley, A.T. (2009) Noncanonical frizzled signaling regulates cell polarity of growth plate chondrocytes. *Development*, **136**, 1083–1092.
  29. Nasevicius, A., Hyatt, T., Kim, H., Guttman, J., Walsh, E., Sumanas, S., Wang, Y. and Ekker, S.C. (1998) Evidence for a frizzled-mediated wnt pathway required for zebrafish dorsal mesoderm formation. *Development*, **125**, 4283–4292.
  30. Niemann, S., Zhao, C., Pascu, F., Stahl, U., Aulepp, U., Niswander, L., Weber, J.L. and Muller, U. (2004) Homozygous WNT3 mutation causes tetra-amelia in a large consanguineous family. *Am. J. Hum. Genet.*, **74**, 558–563.
  31. Brugmann, S.A., Goodnough, L.H., Gregorieff, A., Leucht, P., ten Berge, D., Fuerer, C., Clevers, H., Nusse, R. and Helms, J.A. (2007) Wnt signaling mediates regional specification in the vertebrate face. *Development*, **134**, 3283–3295.
  32. He, F., Xiong, W., Yu, X., Espinoza-Lewis, R., Liu, C., Gu, S., Nishita, M., Suzuki, K., Yamada, G., Minami, Y. et al. (2008) Wnt5a regulates directional cell migration and cell proliferation via Ror2-mediated noncanonical pathway in mammalian palate development. *Development*, **135**, 3871–3879.
  33. Jin, Y.R., Han, X.H., Taketo, M.M. and Yoon, J.K. (2012) Wnt9b-dependent FGF signaling is crucial for outgrowth of the nasal and maxillary processes during upper jaw and lip development. *Development*, **139**, 1821–1830.
  34. Yu, H., Ye, X., Guo, N. and Nathans, J. (2012) Frizzled 2 and frizzled 7 function redundantly in convergent extension and closure of the ventricular septum and palate: evidence for a network of interacting genes. *Development*, **139**, 4383–4394.
  35. Kispert, A., Vainio, S., Shen, L., Rowitch, D.H. and McMahon, A.P. (1996) Proteoglycans are required for maintenance of Wnt-11 expression in the ureter tips. *Development*, **122**, 3627–3637.
  36. Summerhurst, K., Stark, M., Sharpe, J., Davidson, D. and Murphy, P. (2008) 3D representation of Wnt and Frizzled gene expression patterns in the mouse embryo at embryonic day 11.5 (E11.5). *Gene Expr. Patterns*, **8**, 331–348.
  37. Chiquet, B.T., Blanton, S.H., Burt, A., Ma, D., Stal, S., Mulliken, J.B. and Hecht, J.T. (2008) Variation in WNT genes is associated with non-syndromic cleft lip with or without cleft palate. *Hum. Mol. Genet.*, **17**, 2212–2218.
  38. Yao, T., Yang, L., Li, P.Q., Wu, H., Xie, H.B., Shen, X. and Xie, X.D. (2011) Association of Wnt3A gene variants with non-syndromic cleft lip with or without cleft palate in Chinese population. *Arch. Oral Biol.*, **56**, 73–78.
  39. Curtin, E., Hickey, G., Kamel, G., Davidson, A.J. and Liao, E.C. (2011) Zebrafish wnt9a is expressed in pharyngeal ectoderm and is required for palate and lower jaw development. *Mech. Dev.*, **128**, 104–115.
  40. Verkaar, F., van Rosmalen, J.W., Smits, J.F., Blankesteyn, W.M. and Zaman, G.J. (2009) Stably overexpressed human Frizzled-2 signals through the beta-catenin pathway and does not activate Ca<sup>2+</sup>-mobilization in Human Embryonic Kidney 293 cells. *Cell. Signal.*, **21**, 22–33.
  41. Matsumoto, S., Fumoto, K., Okamoto, T., Kaibuchi, K. and Kikuchi, A. (2010) Binding of APC and dishevelled mediates

- Wnt5a-regulated focal adhesion dynamics in migrating cells. *EMBO J.*, **29**, 1192–1204.
42. Albers, J., Schulze, J., Beil, F.T., Gebauer, M., Baranowsky, A., Keller, J., Marshall, R.P., Wintges, K., Friedrich, F.W., Priemel, M. *et al.* (2011) Control of bone formation by the serpentine receptor Frizzled-9. *J. Cell Biol.*, **192**, 1057–1072.
43. Bell, G.W., Yatskevych, T.A. and Antin, P.B. (2004) GEISHA, a whole-mount in situ hybridization gene expression screen in chicken embryos. *Develop. Dyn.*, **229**, 677–687.
44. Darnell, D.K., Kaur, S., Stanislaw, S., Davey, S., Konieczka, J. H., Yatskevych, T.A. and Antin, P.B. (2007) GEISHA: an in situ hybridization gene expression resource for the chicken embryo. *Cytogenet. Genome Res.*, **117**, 30–35.